Surface Functionalization

DOI: 10.1002/anie.201000774

Reversible Self-Assembly of Metal Chalcogenide/Metal Oxide Nanostructures Based on Pearson Hardness**

*Jugal Kishore Sahoo, Muhammad Nawaz Tahir, Aswani Yella, Thomas D. Schladt, Enrico Mugnaoli, Ute Kolb, and Wolfgang Tremel**

Dedicated to Professor Bernd Harbrecht on the occasion of his 60th birthday

Nanotechnology has reached a stage of development where not individual nanoparticles but rather systems of greater complexity are the focus of concern.[1] These complex structures incorporate two or more types of materials, an example of which is the formation of metal–semiconductor hybrids, which effectively combine the properties of both materials.[2] The assembly of multicomponent nanoparticles from constituents with different optical, electrical, magnetic, and chemical properties can lead to novel functionalities that are independent of the individual components and may be tailored to fit a specific application. These applications include such far-reaching challenges as solar energy conversion,[3] biological sensors,[4] mechanical and optical devices,[5] and potential methods for drug delivery and medical diagnostics.[6]

A specific challenge is to assemble nanoparticles into a hierarchical structure. Nanotubes (NT-MQ_2)[7] and fullerenes (IF-MQ_2)[8] of layered metal chalcogenides are the purely inorganic analogues of carbon fullerenes and nanotubes, and exhibit analogous mechanical[9] and electronic properties.[10] They consist of metal atoms sandwiched between two inert chalcogenide layers. Their physical properties[11] are related to their crystal structures, which contain MQ_2 slabs with metal atoms sandwiched between two inert chalcogen layers. These MQ_2 layers are stacked with only van der Waals contacts between them. The steric shielding of the metal atoms by the chalcogen surface layers from nucleophilic attack by oxygen or organic ligands makes chalcogenide nanoparticles highly inert and notoriously difficult to functionalize.

Some progress has been made by employing chalcophilic transition metals in combination with multidentate surface ligands: The 3d metals "wet" the sulfur surface of the chalcogenide nanoparticles whilst the multidentate surface ligands partially block one hemisphere of the metal coordination environment. This steric shielding prevents an aggregation of the chalcogenide nanoparticles through interparticle cross-linking.[12]

The assembly of aggregates from different types of nanoparticles typically relies on chemical modifications of the nanoparticle surface to achieve a specific linkage. A bifunctional organic linker molecule having specific anchor groups for each type of nanoparticle is bound with one of its anchor groups to the first type of the pre-synthesized nanoparticles. In a subsequent step, the second anchor group is used for the attachment of the second type of nanoparticles.[13]

The goal is to attach a controlled number of target molecules while avoiding aggregation through nonspecific interactions with surfaces and other particles in solution. To achieve that goal, the nanoparticles have to be stabilized with a protecting layer containing some chemical anchor points for further modification. This covalent chemical attachment offers high stability in different solvents and ionic environments. Therefore, current strategies for the functionalization of nanoparticles rely on either 1) non-covalent physisorption of linker molecules to the surface of the nanoparticles,[14] 2) electrostatic anchoring of an additional polymeric layer,[15] or 3) the use of short bifunctional cross-linkers. These processes lead to low yields[16] or low surface coverage.[17]

An alternative strategy is to grow nanoparticles directly on the nanotubes by using colloidal nanoparticle synthesis methods.[18] Colloidal nanoparticles may have an affinity based on their acid–base properties, functional groups, or Pearson hardness[19] for nanotube surfaces that allows their attachment without the aid of linkers.

Herein we present a novel synthetic strategy based on Pearson's HSAB (hard/soft acid–base) principle.[19c] that allows the formation of a hierarchical assembly of metal chalcogenide/metal oxide nanostructures. The metal oxide particles can be functionalized in a subsequent reaction step at room temperature to tailor the chalcogenide surfaces or to reversibly detach them from the chalcogenide surfaces with excess surface ligand (Scheme 1). The recycled chalcogenide

---

[*] J. K. Sahoo, Dr. M. N. Tahir, Dr. A. Yella, T. D. Schladt,
Prof. Dr. W. Tremel
Institut für Anorganische Chemie und Analytische Chemie der
Johannes Gutenberg Universität
Duesbergweg 10–14, 55099 Mainz (Germany)
Fax: (+49) 6131-39-25605
E-mail: tremel@uni-mainz.de

Dr. E. Mugnaoli, Dr. U. Kolb
Institut für Physikalische Chemie
Johannes Gutenberg Universität
Welderweg 11, 55099 Mainz (Germany)

[**] This work was supported by the Deutsche Forschungsgemeinschaft (DFG) within the priority program 1165 "Nanotubes and Nanowires: From Controlled Synthesis to Function" (research program: "From single molecules to nanoscopically structured materials"). A.Y. is a recipient of a fellowship from POLYMAT, the Graduate School of Excellence of the State of Rhineland-Palatinate. T.D.S. is a recipient of a Carl Zeiss Fellowship. We acknowledge support for the Electron Microscopy Center in Mainz (EZMZ) from the Center for Complex Matter (COMATT).

Supporting information for this article is available on the WWW under http://dx.doi.org/10.1002/anie.201000774.

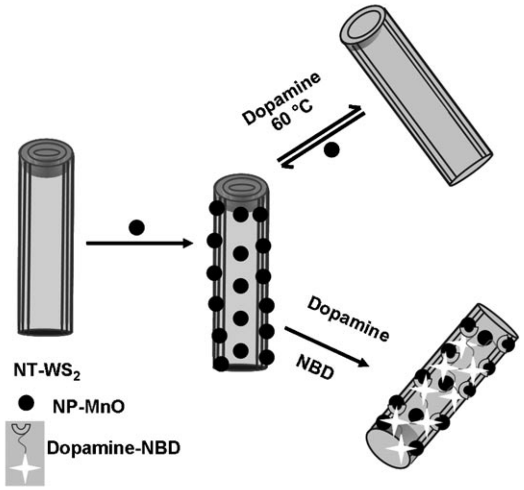

Scheme 1. Representation of reversible immobilization of MnO NPs on NT-WS$_2$ and surface functionalization with fluorophore-labeled dopamine.

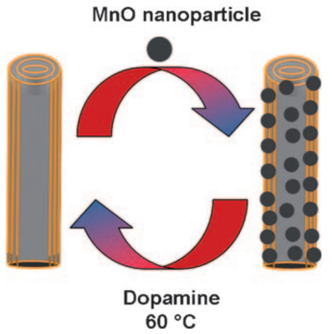

Scheme 2. The reversible functionalization of MnO NPs on NT-WS$_2$.

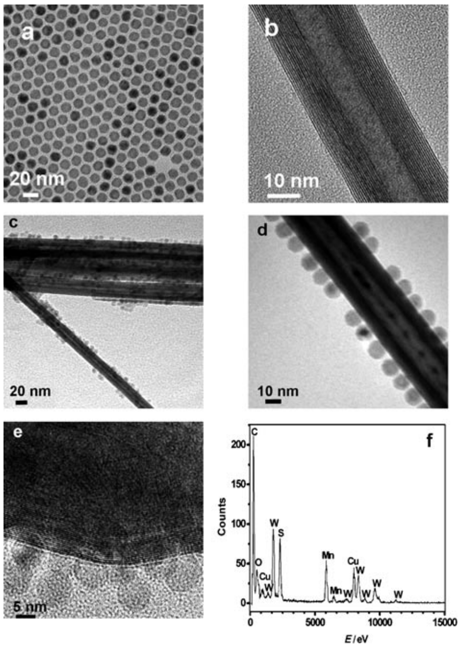

Figure 1. TEM images of the as-synthesized a) MnO NPs and b) NT-WS$_2$. c–e) The attachment of MnO NPs onto NT-WS$_2$. c) TEM overview image, d,e) HRTEM image of the interface of MnO NPs and sidewalls (d) or the tip (e) of a WS$_2$ nanotube. f) EDX spectrum of the MnO@NT-WS$_2$ nanocomposite.

nanoparticles can be used time and again without the use of organic ligands (Scheme 2).

According to Pearson's HSAB principle, a hard Lewis acid has a tendency to bind with a hard Lewis base, and a soft acid with a soft base.[19c] Thus, in the layered metal chalcogenides the soft sulfur surface layer has a tendency to bind with other nanoparticles containing soft transition metal cations. The components chosen to build these magnetic nanohybrids, MnO nanoparticles (MnO NPs) and WS$_2$ nanotubes (NT-WS$_2$), were prepared separately in the first step. Figure 1 a,b show representative transmission electron microscopy (TEM) images of these building blocks, which were synthesized according to published procedures.[20] As the MnO NPs carry oleic acid molecules as surface ligands, they are soluble in most organic solvents (cyclohexane, toluene, or THF).[20a] The NT-WS$_2$ were prepared by the sulfidization of WO$_3$ nanorods obtained by hydrothermal synthesis.[20b] A HR (high-resolution) TEM image of one such NT-WS$_2$ is shown in Figure 1 b. The interlayer spacing between the tubular walls (0.65 nm) is consistent with the (002) d spacing of the 2H-WS$_2$ lattice.

The assembly of oxide/chalcogenide nanostructures was produced by mixing dispersions of the chalcogenide nanoparticles and metal oxide nanoparticles in toluene by mechanical shaking. During this process, the metal oxide nanoparticles were assembled onto the chalcogenide nanoparticle surface by ligand exchange. In this process, the oleic acid capping ligands on the surface of the oxide nanoparticles are substituted by the surface sulfur atoms of the chalcogenide nanoparticles. The binding of MnO NPs to NT-WS$_2$ is illustrated in the TEM images in Figure 1 c–e along with energy-dispersive X-ray analysis (EDX; Figure 1 f). The soft basic character of the chalcogenide surface is of prime importance for the surface binding. The chemisorption of ions or molecules involves their acidic or basic properties, which have to be opposite to those of the active surface sites. The overview TEM image (Figure 1 c) shows that almost all the nanotubes are covered with MnO nanoparticles, and a HRTEM image shows that almost all nanoparticles are sitting on the basal plane of nanotubes. A scanning electron microscopy (SEM) image (Supporting Information, Figure S2) also gives an overview to confirm the immobilization of MnO NPs on NT-WS$_2$. EDX of the composite nanotubes (Figure 1 f) indicates the presence of the elements W, S, Mn, and O. The analytical data indicate a significant amount of MnO NPs present on the surface of the NT-WS$_2$, in accordance with the results of the TEM study.

As described earlier, the tailoring of the chalcogenide surfaces is difficult and requires some suitable approaches, whereas the metal oxide surfaces are easy to functionalize. The MnO NPs surface-bound to NT-WS$_2$ therefore allow the selective functionalization. In this process, the oleic acid capping ligands are replaced by free catechol ligands.

Figure 2 a shows the UV/Vis spectrum of the MnO@NT-WS$_2$ nanocomposites (black line) and also MnO@NT-WS$_2$ modified with dopamine bound 7-nitrobenzofurazan (NBD)

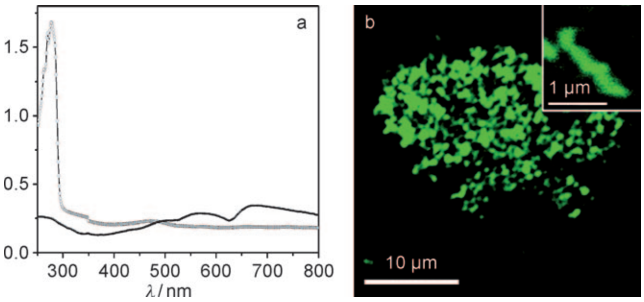

Figure 2. a) UV/Vis absorption spectrum of as-synthesized WS_2 NPs (black line) and MnO@NT-WS_2 nanocomposites functionalized with dopamine-NBD (gray line/○). b) Confocal laser scanning microscopy images of NT-WS_2 coated with NBD-functionalized MnO NPs. Inset: a single nanotube. A 40× oil immersion objective (NA 1.25) was used for the imaging.

dye (gray line/○). A characteristic broad absorption band of WS_2 can be observed at about 660 nm, and the absorption band due to NBD appears at 490 nm, along with a pronounced maximum at 280 nm, which is probably due to excitation of the phenyl ring of the dopamine. The 660 nm absorption band of functionalized NT-WS_2 is weakly visible in the MnO@NT-WS_2 composite. The surface decoration of NT-WS_2 with NBD-functionalized MnO NPs was further demonstrated using confocal laser scanning microscopy (CLSM; Figure 2b). A 10 µL droplet of the sample in THF was placed and dispersed carefully on a thin glass slide, and the solvent was then evaporated. The fluorescence of the NBD dye was excited at 514 nm and detected from 520–540 nm. The overview image of the MnO@NT-WS_2 nanocomposite as-functionalized with NBD ligands (Figure 2b) shows anisotropic fluorescence images of nearly isolated nanoparticles. From the fluorescence images, it is reasonable to conclude that the nanotubes are fully coated with surface-functionalized MnO NPs covalently tethered to the NT-WS_2 surface. It is difficult to comment on the actual size of the functionalized nanotubes because they are below the resolution limits of CLSM. In a control experiment, no fluorescence was observed by exciting the unfunctionalized MnO NPs or unfunctionalized NT-WS_2.

Pearson's HSAB principle states that because of both their thermodynamic and kinetic properties, hard acids prefer to coordinate with hard bases and soft acids with soft bases. The effect of solvation of ions must however be taken into consideration to gain a proper understanding of the HSAB principle. Due to their chelating properties, catechol-type ligands can compete successfully with sulfur for 3d surface metal atoms. As solvation increases with an increase in temperature, we used a temperature of 60 °C to remove all surface-bound MnO NPs from the NT-WS_2 surface in the presence of dopamine as chelating ligand for the metal oxide nanoparticle surfaces. However, without addition of dopamine, it is not possible to reversibly recover the metal chalcogenide nanotubes.

Another reason for the stability of the catecholate surface complexes is valence taumerism of redox-active ligands and transition metal ions. Catecholate ligands form unstrained and unsaturated five-membered-ring chelate systems with surface metal atoms via negatively charged oxygen atoms. Complexes with non-innocent electroactive ligands may exhibit a reversible intramolecular electron transfer between the metal ions and the ligand, leading to a stabilization through internal charge redistribution (Supporting Information, Scheme S2).[21]

Scheme 2 illustrates the attachment and detachment of MnO NPs to NT-WS_2. Whereas oxides of soft and borderline metals are chemisorbed easily to the sulfur surface atoms, oxides of the hard metals have a much lower tendency for binding. In contrast, the catechol-type ligands bind efficiently to hard or borderline metals (such as Ti^{4+}, Fe^{3+}, Al^{3+}, Mn^{2+}). As a result, the binding of chalcogenide nanoparticles and catechol-type ligands to surface metal atoms of borderline metal oxides is a dynamic equilibrium reaction, the position of which depends on the reactants and temperature. By increasing the reaction temperature to 60 °C, catechol is a preferred surface ligand for the metal oxide particles. It displaces the surface sulfur atoms of NT-WS_2, leaving unfunctionalized NT-WS_2 nanotubes behind. Adding fresh metal oxide nanoparticles to NT-WS_2 leads to a partial replacement of the oleate surface ligands by the surface sulfur atoms of NT-WS_2 and a concomitant binding of metal oxide nanoparticles to NT-WS_2. This cycle can be repeated several times. The recycled chalcogenide nanoparticles can then be re-used (Scheme 3).

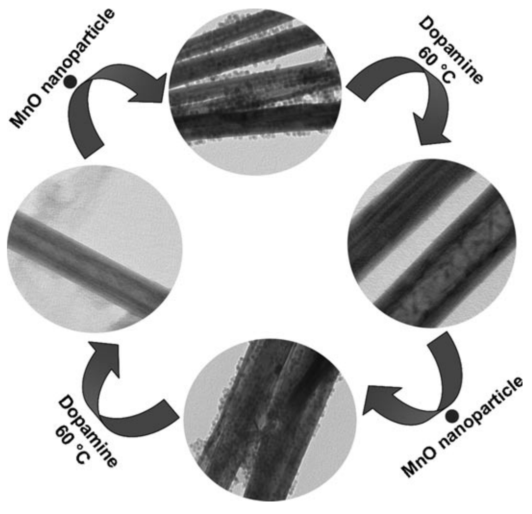

Scheme 3. Reversible attachment of MnO Nps on NT-WS2 and surface modification with fluorophore-labeled dopamine.

The HSAB model has its basis in arguments related to bonding strengths. It is applied to systems where kinetic control, entropy of adduct formation, solvation effects (enthalpic and entropic), ion-pairing effects (enthalpic and entropic), or lattice energy effects (enthalpic and entropic) are large and even dominant. When HSAB considerations are employed, it is implied that the soft–soft (covalent) or hard–hard (ionic) interactions dominate the chemistry; that is, that the reactions are either orbital- or charge-controlled.[22]

In summary, we have used the principles of coordination chemistry to achieve the reversible functionalization of highly inert chalcogenide nanotubes (NT-WS_2) with metal oxide nanoparticles (MnO NPs). The modification strategy is based on the chalcophilic affinity of Mn^{2+}, as described by the Pearson HSAB concept. The surface-bound nanoparticles are still amenable to functionalization with anchor ligands, such dopamine. As the chelating dopamine ligand is a much more potent ligand for surface 3d metals than the sulfur atoms of the chalcogenide nanoparticles, the MnO NPs can be detached from the chalcogenide surface at a slightly elevated temperature. The remaining chalcogenide particles can be the functionalized again with fresh metal oxide nanoparticles.

The self-assembled hybrid architecture can incorporate various different selective nanoparticle–substrate interactions based on well-known surface processes, and it may be generalized for various layered chalcogenide nanoparticles and transition metal and main group oxides. This assembly technique also offers benefits for low-cost and low-waste manufacturing; such methods are becoming increasingly important in the development of green nanofabrication strategies.

The functionalization of WS_2 nanotubes opens several new fields for this class of materials, which have been pursued actively during the past few years for the related carbon nanotubes and various oxide materials: 1) the functionalization of chalcogenide nanotubes for the attachment of electronically active components (metal and semiconductor nanoparticles, light-harvesting ligands for solar-cell applications) to the sidewalls of the tubes; 2) dispersion of nanotubes, for example, for the integration in composites, which is of interest because of their exceptional mechanical properties; and furthermore, it allows 3) the fabrication of thin films by surface binding of chalcogenide particles to oxide surfaces, which might allow their use as lubricants on seemingly incompatible ceramic materials.

Received: February 8, 2010
Revised: April 26, 2010

Keywords: chalcogenides · HSAB principle · MnO nanoparticles · surface functionalization · WS_2 nanotubes

---

[1] a) P. D. Cozzoli, T. Pellegrino, L. Manna, *Chem. Soc. Rev.* **2006**, *35*, 1195; b) H. Zeng, S. Sun, *Adv. Funct. Mater.* **2008**, *18*, 391; c) J. A. McGuire, J. Joo, J. M. Pietryga, R. Schaller, V. I. Klimov, *Acc. Chem. Res.* **2008**, *41*, 1810.
[2] a) V. Subramanian, E. E. Wolf, P. V. Kamat, *J. Phys. Chem. B* **2003**, *107*, 7479; b) T. Mokari, E. Rothenberg, I. Popov, R. Costi, U. Banin, *Science* **2004**, *304*, 1787; c) T. Mokari, C. G. Sztrum, A. Salant, E. Rabani, U. Banin, *Nat. Mater.* **2005**, *4*, 855; d) D. V. Talapin, H. Yu, E. V. Shevchenko, A. Lobo, C. B. Murray, *J. Phys. Chem. C* **2007**, *111*, 14049; e) J. Yang, H. I. Elim, Q. Zhang, J. Y. Lee, W. Ji, *J. Am. Chem. Soc.* **2006**, *128*, 11921.
[3] A. Rizzo, C. Nobile, M. Mazzeo, M. De Giorgi, A. Fiore, L. Carbone, R. Cingolani, L. Manna, G. Gigli, *ACS Nano* **2009**, *3*, 1506.
[4] a) K. Sudeep, S. T. S. Joseph, K. G. Thomas, *J. Am. Chem. Soc.* **2005**, *127*, 6516; b) X. Huang, I. H. El-Sayed, W. Qian, M. A. El-Sayed, *J. Am. Chem. Soc.* **2006**, *128*, 2115.
[5] a) M. Thomalla, H. Tributsch, *J. Phys. Chem. B* **2006**, *110*, 12167; b) J.-P. Salvetat, J.-M. Bonard, N. H. Thomson, A. J. Kulik, L. Forrö, W. Benoit, L. Zuppiroli, *Appl. Phys. A* **1999**, *69*, 255.
[6] a) I. Gorelikov, L. M. Field, E. Kumacheva, *J. Am. Chem. Soc.* **2004**, *126*, 15938; b) A. K. Salem, P. C. Searson, K. W. Leong, *Nat. Mater.* **2003**, *2*, 668; c) M. I. Shukoor, F. Natalio, P. Gupta, M. N. Tahir, H. A. Therese, S. Weber, S. Fischer, N. Metz, P. Theato, L. M. Schreiber, H. C. Schröder, W. E. G. Müller, W. Tremel, *Adv. Funct. Mater.* **2009**, *19*, 3717.
[7] a) L. Margulis, G. Salitra, R. Tenne, M. Talianker, *Nature* **1993**, *365*, 113; b) A. Yella, E. Mugnaioli, M. Panthöfer, H. A. Therese, U. Kolb, W. Tremel, *Angew. Chem.* **2009**, *121*, 6546; *Angew. Chem. Int. Ed.* **2009**, *48*, 6426.
[8] a) Y. Feldman, E. Wasserman, D. J. Srolovitz, R. Tenne, *Science* **1995**, *267*, 222; b) R. Tenne, M. Homyonfer, Y. Feldman, *Chem. Mater.* **1998**, *10*, 3225; c) W. Tremel, *Angew. Chem.* **1999**, *111*, 2311; *Angew. Chem. Int. Ed.* **1999**, *38*, 2175.
[9] a) Y. R. Hacohen, E. Grunbaum, R. Tenne, J. Sloan, J. L. Hutchison, *Nature* **1998**, *395*, 336; b) A. Q. Zhu, T. Sekine, Y. H. Li, W. X. Wang, M. Y. Fay, H. Edwards, P. D. Brown, N. Fleischer, R. Tenne, *Adv. Mater.* **2005**, *17*, 1500; c) I. Kaplan-Ashiri, S. R. Cohen, K. Gartsman, R. Rosentsveig, V. Ivanovskaya, T. Heine, G. Seifert, H. D. Wagner, R. Tenne, *Proc. Natl. Acad. Sci. USA* **2006**, *103*, 523.
[10] a) L. Scheffer, R. Rosentzveig, A. Margolin, R. Popovitz-Biro, G. Seifert, S. R. Cohen, R. Tenne, *Phys. Chem. Chem. Phys.* **2002**, *4*, 2095; b) M. Nath, S. Kar, A. K. Raychaudhuri, C. N. R. Rao, *Chem. Phys. Lett.* **2003**, *368*, 690.
[11] a) F. Hulliger, *Structural Chemistry of the Layer-Type Phases* (Ed.: F. Levy), Reidel, **1976**; b) A. Katz, M. Redlich, L. Rapoport, H. D. Wagner, R. Tenne, *Tribol. Lett.* **2006**, *21*, 135.
[12] a) M. N. Tahir, M. Eberhardt, N. Zink, H. A. Therese, U. Kolb, P. Theato, W. Tremel, *Angew. Chem.* **2006**, *118*, 4927; *Angew. Chem. Int. Ed.* **2006**, *45*, 4809; b) M. N. Tahir, N. Zink, M. Eberhardt, H. A. Therese, U. Kolb, P. Theato, W. Tremel, *Small* **2007**, *3*, 829; c) M. N. Tahir, M. Eberhardt, P. Theato, S. Faiß, A. Janshoff, T. Gorelik, U. Kolb, W. Tremel, *Angew. Chem.* **2006**, *118*, 922; *Angew. Chem. Int. Ed.* **2006**, *45*, 908; d) M. N. Tahir, M. Eberhardt, H. A. Therese, U. Kolb, P. Theato, W. E. G. Mueller, H. C. Schroeder, W. Tremel, *Angew. Chem.* **2006**, *118*, 4921; *Angew. Chem. Int. Ed.* **2006**, *45*, 4803; e) M. N. Tahir, F. Natalio, H. A. Therese, A. Yella, N. Metz, M. R. Shah, E. Mugnaioli, R. Berger, P. Theato, H. C. Schroeder, W. E. G. Müller, W. Tremel, *Adv. Funct. Mater.* **2009**, *19*, 285; f) M. N. Tahir, A. Yella, H. A. Therese, E. Mugnaioli, M. Panthöfer, H. U. Khan, W. Knoll, U. Kolb, W. Tremel, *Chem. Mater.* **2009**, *21*, 5382.
[13] a) I. Robel, B. A. Bunker, P. V. Kamat, *Adv. Mater.* **2005**, *17*, 2458; b) S. Banerjee, S. S. Wong, *Nano Lett.* **2002**, *2*, 195; c) L. Sheeney-Haj-Ichia, B. Basnar, I. Willner, *Angew. Chem.* **2005**, *117*, 80; *Angew. Chem. Int. Ed.* **2005**, *44*, 78.
[14] D. Spetzler, J. York, D. Daniel, R. Fromme, D. Lowry, W. Frasch, *Biochemistry* **2006**, *45*, 3117.
[15] A. Gole, C. J. Murphy, *Langmuir* **2005**, *21*, 10756.
[16] B. F. Pan, L. M. Ao, F. Gao, H. Y. Tian, R. He, D. X. Cui, *Nanotechnology* **2005**, *16*, 1776.
[17] a) J. Y. Chang, H. Wu, H. Chen, Y. C. Ling, W. Tan, *Chem. Commun.* **2005**, 1092; b) K. K. Caswell, J. N. Wilson, U. H. F. Bunz, C. J. Murphy, *J. Am. Chem. Soc.* **2003**, *125*, 13914; c) A. K. Salem, M. Chen, J. Hayden, K. W. Leong, P. C. Searson, *Nano Lett.* **2004**, *4*, 1163.
[18] a) M. Olek, T. Busgen, M. Hilgendorff, M. Giersig, *J. Phys. Chem. B* **2006**, *110*, 12901; b) S. Banerjee, S. S. Wong, *Chem. Commun.* **2004**, 1866; c) B. H. Juárez, C. Klinke, A. Kornowski,

H. Weller, *Nano Lett.* **2007**, *7*, 3564; d) Y. J. Na, H. S. Kim, J. J. Park, *J. Phys. Chem. C* **2008**, *112*, 11218.

[19] a) R. G. Pearson, *J. Am. Chem. Soc.* **1963**, *85*, 3533; b) R. G. Pearson, *Chemical Hardness. Applications from Molecules to Solids*, Wiley-VCH, Weinheim, **1997**; c) F. Umland, G. Wünsch, *Charakteristische Reaktionen Anorganischer Stoffe*, 2nd ed., Aula Verlag, Wiesbaden, **1991**.

[20] a) T. D. Schladt, T. Graf, W. Tremel, *Chem. Mater.* **2009**, *21*, 3183; b) H. A. Therese, J. Li, U. Kolb, W. Tremel, *Solid State Sci.* **2005**, *7*, 67; c) J. Etzkorn, H. A. Therese, F. Rocker, N. Zink, U. Kolb, W. Tremel, *Adv. Mater.* **2005**, *17*, 2372.

[21] a) The associated valence tautomerism has been studied in depth for molecular compounds. First, they are unique model systems that provide insight into the basic factors affecting intramolecular electron transfer in coordination complexes. Second, from an applied perspective, the large changes in the optical, structural, and magnetic properties that often accompany valence tautomeric interconversion have potential applications in bistable molecular switching materials and devices. See: b) C. G. Pierpont, C. W. Lange, *Prog. Inorg. Chem.* **1994**, *41*, 331; c) P. Gütlich, A. H. Hauser, H. Spiering, *Angew. Chem.* **1994**, *106*, 2109; *Angew. Chem. Int. Ed. Engl.* **1994**, *33*, 2024.

[22] a) G. Klopman, *J. Am. Chem. Soc.* **1968**, *90*, 223; b) L. Salem, *J. Am. Chem. Soc.* **1968**, *90*, 543; c) L. Salem, *J. Am. Chem. Soc.* **1968**, *90*, 553; d) M. Klessinger, *Elektronenstructur organischer Moleküle: Grundbegriffe quantumchemischer Betrachtungsweisen*, Verlag Chemie, Weinheim, **1982**.